Title

Genetic variation and radiation quality impact cancer promoting cellular phenotypes in response to HZE exposure

Authors

Sridharan, Deepa M
Enerio, Shiena
Wang, Chris
et al.

Publication Date

2019-02-01

DOI

10.1016/j.lssr.2018.10.002

Peer reviewed

Genetic variation and radiation quality impact cancer promoting cellular phenotypes in response to HZE exposure

Deepa M. Sridharan[a], Shiena Enerio[b], Chris Wang[b], Mark A. LaBarge[c], Martha R. Stampfer[b], Janice M. Pluth[d,*]

[a] Division of Chemical Sciences, Lawrence Berkeley National Laboratory, Berkeley, CA 94803, USA
[b] Division of Biological Systems and Engineering, Department of BioEngineering & BioMedical Sciences, Lawrence Berkeley National Laboratory, Berkeley, CA 94803, USA
[c] Department of Population Sciences, City of Hope National Medical Center, Duarte, CA 91010, USA
[d] Department of Health Physics and Diagnostic Sciences, University of Nevada Las Vegas, Las Vegas, NV 89154, USA

A B S T R A C T

There exists a wide degree of genetic variation within the normal human population which includes disease free individuals with heterozygote defects in major DNA repair genes. A lack of understanding of how this genetic variation impacts cellular phenotypes that inform cancer risk post heavy ion exposure poses a major limitation in developing personalized cancer risk assessment astronauts. We initiated a pilot study with Human Mammary Epithelial Cell strains (HMEC) derived from wild type, a p16 silenced derivative of wild type, and various genetic variants that were heterozygote for DNA repair genes; BRCA1, BRCA2 and ATM. Cells strains were exposed to different high and low LET radiation qualities to generate both simple and complex lesions and centrosome aberrations were examined as a surrogate marker of genomic instability and cancer susceptibility post different exposures. Our results indicate that centrosome aberration frequency is higher in the genetic variants under study. The aberration frequency increases with dose, complexity of the lesion generated by different radiation qualities and age of the individual. This increase in genomic instability correlates with elevated check-point activation post radiation exposure. These studies suggest that the influence of individual genetics on cell cycle regulation could modify the degree of early genomic instability in response to complex lesions and potentially define cancer predisposition in response to HZE exposure. These results will have significant implications in estimating cancer susceptibility in genetically variant individuals exposed to HZE particles.

1. Introduction

Astronauts traveling in space are exposed to high charge high energy (HZE) ions that can generate multiple lesions, including DSBs, within a single turn of the DNA helix. While redundancies in DNA repair mechanisms (Aparicio et al., 2014; Karran, 2000) effectively remove some of these complex lesions, commonly referred to as clustered damages, those that remain unrepaired or are mis-repaired can cause local and global genome rearrangements that threaten both the integrity of the genome and potentiate long term cancer risk (Stephens 2011;Gudowska, 2004). *BRCA1, BRCA2, ATM and p16* are four key genes that play central roles in the maintenance of genomic integrity by coordinating a delicate balance between DNA repair processes and cell cycle checkpoint activation. Their broad function as tumor suppressors is underscored by the fact that germ line mutations in these genes have been shown to confer an increased susceptibility to different types of cancer (Walsh et al., 2016;Dilworth, 2000; Ahmed & Rahman, 2006).

ATM is one of the first responders to radiation-induced DNA damage and orchestrates repair response by phosphorylating chk2 (Matsuoka et al., 2000) and other downstream substrates involved in checkpoint control, repair, and apoptosis (Falck et al., 2001, Zhou and Elledge, 2000). Consequently, ATM deficient cells exhibit pronounced radiosensitivity, failure to initiate cell cycle checkpoints and chromosome instability in response to radiation exposure (Kuhne et al., 2004). BRCA1 is one of the key repair substrates of ATM that is quickly recruited to DNA lesions and participates in DNA repair through association with a number of proteins including Rad51. Essential roles in numerous pathways including activation and repression of

Abbreviations: HZE, High charge high energy; DSB, Double strand break; WT, Wild Type; HMEC, Human Mammary Epithelial Cells; DDR, DNA damage response; MFI, Mean fluorescence intensity; LET, Linear energy transfer; PBS, Phosphate buffered saline

* Corresponding author.
E-mail address: Janice.Pluth@unlv.edu (J.M. Pluth).

transcription, homologous recombination (HR), cell cycle regulation, check point activation, DNA damage repair, protein ubiquitination, chromatin remodeling, and apoptosis have been attributed to BRCA1 (Moynahan et al., 1999). In contrast to the multifaceted role of BRCA1, the main role of BRCA2 is to regulate the proficiency of repair and recombination processes and maintaining genomic instability by controlling the enzymatic activity of RAD51 (Davies et al., 2001). The importance of both BRCA1 and BRCA2 in HR is well documented by the aberrant chromosomal structures and radiosensitivity observed in cells with defects in these proteins (Patel et al., 1998; Moynahan et al., 1999; Xu et al., 1999). p16 is a tumor suppressor that functions by inhibiting the progression from G1 to S phase in response to cellular stresses such as radiation [Shapiro, 1998]. This is an essential step in the initiation and maintenance of a stress-associated senescence barrier termed stasis; the first barrier that limits proliferation potential to prevent immortalization (Garbe et al., 2007). It has been shown that stasis is accompanied by increased levels of p16 and can be bypassed by loss of p16 expression, a phenotype frequently observed in human breast cancer (Brenner et al., 1996). These studies highlight the distinct roles of ATM, BRCA1, BRCA2 and p16 in the cellular response to double strand breaks.

Numerous mutations and polymorphisms have been reported in BRCA1, BRCA2 and ATM (Karami and Mehdipour, 2013); Choi, 2016]. Mutations in one copy of BRCA1, BRCA2 or ATM have been noted in ~0.26–0.32%, ~0.36%, and ~0.50–1.50% of the general population respectively (Broeks et al., 2000, Mann et al., 2006, Maxwell et al., 2016, Swift et al., 1986). While some of these cause nonsynonymous sequence alterations that adversely affect function and promote carcinogenesis, the impact of others are either silent, or in some cases even been speculated to have a protective role in preventing breast cancer development (Karami and Mehdipour, 2013). Of interest, rare cells with spontaneous dysfunction of p16, similar to the phenotype observed in cancer cells, have also been observed in vivo within normal tissue of some women (Brenner et al., 1998, Holst et al., 2003, McDermott et al., 2006). However studies on whether these variants confer increased cancer risk and differ in their biological response to cell stressors have been controversial.

It is likely that the astronaut cohort could include some of these genetic variants. To provide personalized risk assessments for astronauts, NASA has undertaken a monumental effort to factor-in the weights of various variables such as age, gender and tobacco-use, on the risk of developing cancer from space radiation exposure. Thus far genetic variation has not been used modeling cancer risk from space radiation exposure. However, as disease-free heterozygote individuals with defects in major DNA repair genes exist within the normal population, a better understanding of how this impacts cancer development processes at early times post HZE exposure would lay the groundwork for potentially using genetic variation in informing cancer risk assessments in astronauts.

To test whether genetic variation had an impact on early response to lesions that differ in complexity, we undertook a small scale study by comparing a subset of human mammary epithelial cell strains (HMECs) derived from individuals who are genetic variants, namely heterozygous for BRCA1, BRCA2 and ATM and compared them to a wild type strain with and without knock down of p16 expression using short hair pin RNA (shRNA) against p16, which allowed us to examine the damage response phenotype when the stasis barrier is impacted. We exposed HMECs to two different doses of high and low Linear energy transfer (LET) radiation and compared the frequency of centrosome aberrations elicited, as a useful surrogate marker to predict genome instability, at different times post radiation exposure. In the second part of this study, as drivers of centrosome duplication in radiation induced carcinogenesis are unclear, we tested the hypothesis that early DNA Damage Response (DDR) that impacts checkpoint regulation may predict strain specific changes in centrosome numbers and resulting genomic instability. Herein we compared centrosome aberration frequency to the degree of expression and activation of key proteins involved in checkpoint regulation. Our results suggest that genetic variants exhibit increased numbers of centrosome aberrations following exposure to complex damages in comparison to simple damages, induced by high vs low LET radiation respectively. Elevation of key nodes in check point regulation such as pChk1, pChk2, p53 and ATR appear to parallel the increase in centrosome aberration frequency.

2. Materials and methods

2.1. Cell strains

We have utilized primary HMEC strains derived from normal and heterozygote carriers for various DNA repair proteins involved in breast cancer risk. These include Wild Type (WT) specimen 184D, derived from a 21y old individual; specimen 90P derived from a non-tumor mastectomy from a 36y old BRCA1(+/−) individual; specimen 255 L derived from a prophylactic mastectomy from a 30y old BRCA2(+/−) individual and specimen 245AT derived from a prophylactic mastectomy from a 41y old ATM (+/−). The study was limited to one strain for each gene, owing to the availability of only these strains in the HMEC Bank at the time of study, and the necessity to maintain uniformity in strain isolation and culture conditions. To compare the effect of p16 silencing, that is sporadically observed as part of malignant progression, the WT 184D strain was compared to its genetically modified post-stasis derivative, wherein p16 was silenced by retroviral transduction of p16 shRNA without introducing gross genomic errors (Garbe et al., 2014). A subset of six primary WT HMEC strains chosen from a wider cohort of individuals of different ages that were used in our previous study (Sridharan et al., 2017), were used to examine the impact of radiation quality on age dependent genomic instability. These included two pre-stasis strains chosen from individuals in three distinct age groups: (young: specimen 48R (16y) and 240 L (19y); middle-age: specimen 60R (47y) and 030 (49y) and old: specimen 71C (65y) and specimen 122 L (66y). These strains were exposed to a low and high dose of 93 MeV/u Silicon ions and compared with the same strains exposed to 300 MeV/u Titanium ions. Samples were processed 9 days post exposure. Early passages of these finite-lifespan strains were grown from a large bank of frozen organoids as described (Garbe et al., 2009, Labarge et al., 2013). Details on the derivation and culture of these HMECs can be found on the HMEC Bank website, http://hmec.lbl.gov. All experiments were performed in accordance with relevant guidelines and regulations approved by Lawrence Berkeley National Laboratory Human Subjects Committee, IRB protocols 305H002 and 108H004. The HMEC specimens used in this study were obtained between 1977 and 1981. This was before the current IRB consent regulations were in place. Consent at that time was covered by the hospitals' consent forms which gave the pathologists permission to use or distribute discarded surgical material (which is what was obtained) at their discretion. Our current IRB protocols (305H002 and 108H004) explicitly allows us to distribute and use this material.

2.2. Cell culture

Cell strains were obtained from the HMEC bank at 2nd passage (P2) and were subsequently passaged to generate the required number of P4 cell stock vials at 1 × 10^6 million cells per ml, for use in all experiments. 4th passage HMEC strains were seeded at the same number for all strains and grown to sub-confluence (85%confluency ~ 0.5 × 10^6 cells) in T75 flasks and exposed to radiation. Serum-free M87A medium supplemented with 0.5 ng/ml cholera toxin (CT), and 0.1 nM oxytocin (Bachem) (Garbe et al., 2009) was used to replace the media in culture flasks every two days and strains were routinely tested for absence of mycoplasma contamination (Bionique Test Labs, NY), prior to use.

2.3. Irradiation

Cell strains plated in T75 cm^2 (Corning) flasks were exposed in log phase to different radiation qualities at room temperature. Two parameters that define the unique track structure of heavy ion exposures are LET, defined as the linear energy transferred per unit distance, and Z^2/β^2 where Z is the effective charge number of the particle, which accounts for atomic screening effects, and β the velocity of the particle scaled to the speed of light. Z^2/β^2 is an accepted equivalent of the number and intensity of delta rays generated. Heavy ion exposures Silicon 93 MeV/u (Si93, LET 152 keV/μm, Z^2/β^2 1137) and Titanium 300 MeV/u (Ti300, LET 171 keV/μm, Z^2/β^2 1136) were carried out at the NASA Space Radiation Laboratory (NSRL) at Brookhaven National Laboratory, Upton, NY, and characterized by different LET values but similar Z^2/β^2 values obtained from NSRL. To prevent particle fragmentation, cell culture flasks were placed vertically, perpendicular to the axis of the horizontal beam, oriented with the cell side closest to the beam, as illustrated in the beam profile captured by the digital beam imager at NSRL (https://www.bnl.gov/nsrl/userguide/beam-uniformity-and-profile.php). The beam diameter was 20 × 20 cm^2 square, with a uniform center and variation of +/− 10% at the periphery. Cells were exposed to either a low dose of 0.05 Gy or high dose of 0.5 Gy chosen based on effectiveness of this dose in generating centrosome aberrations as shown previously (Sridharan et al., 2017). Dosimetry calibration at NSRL was carried out using standardized techniques outlined in the NSRL user guide (https://www.bnl.gov/nsrl/userguide/dosimetry-calibration.php). In brief, a small ion chamber called a "Calibration Ion Chamber" (Far West Technology) routinely calibrated using a standard gamma ray source (Cs-137), is mounted on a dual axis drive that allows the remote placement of the device. Once the beam has been tuned, prior to each set of exposures, the Calibration Ion Chamber measures the dose delivered by the beam at the same time as a series of large ion chambers is being read out. This reading serves to transfer the calibration to the large ion chambers that remain in the beam just upstream of the samples during exposures. It is these secondary ion chambers that measure the integrated dose delivered and cut off the beam when the desired dose has been achieved. Dose rates ranging from (0.05–0.06) Gy/min for low dose exposures and (0.22–0.32) Gy/min for high dose exposures were used to maintain short exposure times (0.5–2 min). Both mock irradiated and Si radiation-exposed cells were cultured and processed at 24 h and 72 h following treatment for multiplexed profiling of proteins involved in DNA damage response, and the 72 h sample was used to score centrosome aberrations. An aliquot from both Si 93 and Ti 300 MeV/u exposed samples were shipped to LBNL to subsequently define centrosome aberrations in long-term culture (9 days post exposure).

Cells were exposed to Cesium radiation at Lawrence Livermore National Laboratory at dose rates of ~0.12 Gy/min for low doses and ~1.80 Gy/min for high doses and processed similar to the previous samples. For each cell line, flasks were irradiated using a 137Cs Mark 1 Irradiator (J.L. Shepherd and Assoc., Glendale, CA). The negative control was sham irradiated. Slightly higher doses of 0.8 and 0.08 Gy were obtained using 10X and 2X attenuation at dose rates of 0.98 or 0.25 Gy/min, respectively. Based on the known higher effectiveness of high LET radiation, cells were exposed to slightly higher doses for low LET cesium to enable dose comparison within each radiation quality. After irradiation, cells were transferred to 37 °C. TLD dosimeters were used to calculate dosimetry as standard protocol. Before radiation treatment, 2–3 TLDs were blanked and placed in locations flasks would be receiving dose. The measured dose based on TLDs was then defined for flasks that were subsequently irradiated. Two independent flasks were set up for each un irradiated control and dosed sample for each strain. The total number of population doublings for each culture were calculated, using the formula PD = $\log_2$ (recovered viable cell number/number of viable cells seeded)/0.301. The number of population doublings ranged from ~1 to 6 in the radiation exposed samples. The proliferative potential of the pre-stasis strains BRCA1 +/−, BRCA2 +/− and ATM +/− strains in M87A media are known range from ~30 to 50 PD and of the normal strains range from 40 to 60 PD prior to reaching stasis.

2.4. Centrosome aberrations

Cells following exposure to Cs and Si93 MeV/u were detached from flasks on Day 2 with trypsin (5 min. of 0.05% trypsin +5 mM EDTA), following a PBS wash and plated immediately onto a 15 mm round glass German 1.0 coverslip (Fisher scientific Inc.) at a concentration of 0.2×10^5 cells/coverslip for analysis on Day 3. Cells were also seeded at a lower density, 0.5×10^5cells/coverslip for controls and dosed samples, in 60 mm dishes and re-plated onto 15 mm round glass german 1.0 coverslips on Day 8 at 0.2×10^5 cells/ coverslip for analysis 9 days post exposure. Coverslips were fixed in 100% methanol for 10mins at −20 °C, washed in Phosphate Buffered Saline (PBS) and blocked in 1% BSA for 1hr at room temperature (RT). Centrosomes were detected by indirect immunofluorescence, using a primary rabbit antibody against pericentrin (1:1000) (Abcam, Cambridge MA). Following primary antibody incubation (1 h at RT), the cells were washed three times in blocking buffer, and subsequently incubated for 0.5 h with goat anti-rabbit Alexa Fluor 594 (Invitrogen, Waltham MA). Post-secondary antibody incubation, cells were washed twice in PBS, counterstained with 0.1 μg/ml 4′, 6-diamidino-2-phenylindole (DAPI) in PBS, air-dried and mounted with Vectashield (Vector Laboratories, Burlingame, CA). Stained cells were imaged with a Zeiss Axiovert 200M inverted fluorescence microscope equipped with a cooled CDD camera and Image-Pro®Plus software (MediaCybernetics, Rockville MD). Image acquisition was carried out within a week of staining using a 40X air objective.

2.5. Calculation of centrosome aberrations

Centrosome aberrations were scored blind by two independent individuals. Random regions of the slide were imaged for centrosome scoring.For each region scored, we assessed the total number of cells based on DAPI stain, and the number of cells with aberrant centrosomes (> 2 pericentrin foci). Images of cells containing aberrant centrosome numbers were taken at 40X to evaluate the number of centrosomes in each aberrant cell. The majority of the cells in irradiated and unirradiated samples show two pericentrin foci (2P) (Appendix Fig. 7). Cells with supernumerary centrosomes had between 3 to as many as 8 centrosomes, and were scored as aberrant (> 2P).The number of centrosome aberrations per cell were characterized as either 3 centrosomes/cell (3P) or greater than 3 centrosomes/cell (> 3P). The data presented reflect an average of two independent experiments. Between 200 and 400 cells were examined for each sample.

2.6. Multiplex analysis for phospho-protein expression

Two independent samples from each of the strains (WT, WT p16-, BRCA1 +/− and BRCA2 +/−) were exposed to Si93 MeV/u or Cs and examined for the levels of expression of various DNA damage phosphoproteins. The ATM +/− strain was not used in this assay due to lack of sufficient cell numbers. Both irradiated and sham samples were processed 1 and 3 days post radiation exposure. Processing was staggered in batches to ensure quality control. After a cold PBS wash, 300 ul of ice-cold 1X Milliplex lysis buffer (EMD Millipore Inc, MA) with protease inhibitors (Sigma) and phosphatase inhibitors (1 mM sodium orthovanadate, Sigma, MO) was added to each plate on ice. Cells were scraped off the plate, and cell suspensions were transferred to a centrifuge tube and rocked for 15 min at 4C. Particulates were removed by high-speed centrifugation at 12,000 rpm for 10 min at 4C, and protein concentration was determined by bicinchoninic acid assay (BCA assay) using the NanoDrop spectrophotometer (Thermofisher Scientific, DE). Samples were aliquoted and stored at −70C following quantification and prior

to analysis. The MILLIPLEX® MAP 7-plex DNA Damage/Genotoxicity Magnetic Bead kit (EMD Millipore Inc, MA) was used to detect changes in phosphorylated Chk1 (Ser345), Chk2 (Thr68), H2AX (Ser139) and p53 (Ser15) as well as total protein levels of ATR, MDM2 and p21 in cell lysates. 25 µg of sample was used in each well and the immunoassay was carried out according to the published protocol for this kit (48–621 MAG, EMD Millipore Inc, MA) and analyzed using the Luminex® system. Fold changes in overall protein expression or activation were presented per unit dose and were from an average of two independent experiments. Errors bars reflect standard deviation between experi-ments. For each target, the values were background subtracted and normalized to GAPDH levels for each sample

2.7. Statistical analysis

Statistical analysis and testing were carried out using Graph Pad Prism. Two-way ANOVA was used for multiple comparisons of relative centrosome aberration frequency in the variant cell lines compared to the wild type, to estimate the 95% confidence interval. Adjusted p values were obtained using Dunnett's test representing correction for multiple comparisons. Anova was also used for pairwise radiation quality comparison within each cell line and between high and low dose. The following notations have been used in graphs to denote statistical significance; * $= p < 0.05$, ** $= p < 0.01$, and *** $= p < 0.001$. Comparison of differences in the percentage of cells with centrosome aberrations among dosed and unexposed controls were carried out using two tailed t test. Pearson correlation was used to examine the correlation between centrosome aberrations and expression or activation levels of various key nodes in the DNA damage response. Two-way ANOVA was used for multiple comparisons of multiplex data. To correct for false positives with multiple comparisons in multiplexed analysis, both raw p value score (assuming each target was the only one scored) and the adjusted p value calculated using the Bonferroni method, (factoring in the number of targets simultaneously assessed) were obtained to improve the estimates of significance.

3. Results

3.1. Increased centrosome aberrations in cells with genetic variation in DNA damage response genes post exposure to HZE ions

We previously showed that complex damages elicit increased centrosome aberrations in an age dependent manner in HMECs (Sridharan et al., 2017). However, this relationship has not been characterized in HMECs derived from individuals with genetic variations. To address how individual genetics influences the development of surrogate markers of cancer risk, we undertook a pilot study utilizing a small cohort of well-characterized HMEC strains from individuals with single allele mutations in repair genes (BRCA1+/−, BRCA2+/−, ATM+/−), as well as an HMEC strain with or without knock-down of p16 expression (WT, WTP16(-)) by transduction of shRNA to p16 (Garbe et al., 2014).

Pre-stasis 4th passage strains from WT, WTP16(-) and the genetic variants were irradiated with a low (0.05 Gy) and high dose (0.5 Gy) of Si93 MeV/u (Si). Centrosome aberrations 3 days post exposure were compared to Cesium (Cs) exposed samples at similar doses (Fig. 1). The frequency of centrosome aberrations was assessed for two independent experiments. 400 cells were scored for each sample. Aberration frequencies were divided by the number of population doublings (PD) to correct for population doubling differences and normalized to the sham radiated controls. Normalized aberration frequency per unit radiation dose (Gy) was graphed to compare effects at low and high doses. Strain-specific differences in centrosome aberration frequencies were not observed with low dose Cs exposure (Fig. 1A). Relative to WT, centrosome aberration frequencies by the majority of the variant strains were lower with low dose Si 93 MeV/u compared to Cs exposure (Fig. 1A). The BRCA1+/− carrier strain was an exception, exhibiting a higher aberration frequency with low dose Si exposure that was significant ($p < 0.001$) relative to control and relative to the wild type strain WT ($p < 0.05$). As fold changes relative to control were graphed, " * " alone was used to indicate changes relative to sham irradiated controls, and horizontal bars were used to indicate pair-wise comparisons. The ATM+/− strain was not processed following low dose exposure to Si 93 MeV/u due to sample contamination.

When exposed to a high dose of Cs, the BRCA1+/− strain showed the highest frequency of centrosome aberrations in comparison to the other strains, which was significantly ($p < 0.001$) different from its unirradiated control (Fig. 1B). We noted that the centrosome aberration frequencies in the p16 silenced WT strain, ($p < 0.05$), BRCA1+/− ($p < 0.05$), BRCA2+/− and ATM+/− strains were higher with high dose exposure to Si 93 MeV/u in comparison to WT. With high dose exposure, a significant radiation quality difference (Cs Vs Si93) was noted in the p16 silenced WT strain ($p < 0.01$). Interestingly ~2 fold increase is noted in the BRCA1+/− strain relative to the BRCA2+/− strain for both cesium and Si 93 MeV/u exposure. Overall, the genetic variants showed higher frequencies of centrosome aberrations as compared to the WT in response to complex damages induced by Si 93 MeV/u exposure. Of interest, baseline centrosome aberrations in unirradiated samples revealed that centrosome aberrations in the heterozygote strains were also higher than wild type (Appendix Fig. 1). However the aberration frequency of the WTP16(-) strain did not significantly differ from WT.

3.2. Distribution of the number of centrosomes in aberrant cells post Si ion exposure

We next focused on the strains that showed an increase in centrosome aberrations with Si93, to examine whether the type of centrosome aberration was impacted by genetic background. Aberrant cells (> 2 centrosomes) identified while scoring a minimum of 400 cells were classified into two sub-groups; cells with 3 pericentrin foci (3P) and those containing more than 3 pericentrin foci (> 3P). We noted a dose dependent increase in both the 3P and > 3P centrosome subgroups (Fig. 2A and B). With the exception of BRCA1+/− strain where the normalized frequency of aberrant cells containing 3 centrosomes was similar between low and high doses, in all of the other variant strains, the 3P frequency was elevated with high dose as compared to low dose, with ATM+/− exhibiting the highest change (Fig. 2A). However, this increase was not noted in the > 3P population (Fig. 2B), wherein the frequency in the ATM+/− strain was similar to wild type post high dose exposure. We also noted that the BRCA1+/− and the p16 silenced strain showed similar increases in the > 3P population with high dose exposure. Together these results point to some strain specific differences in the distribution of centrosome aberration with HZE exposure.

3.3. Assessment of key nodes involved in check point regulation post DNA damage

Given that cell cycle regulation plays a key role in the maintenance of normal centrosome numbers, we next examined whether proteins involved in check point activation could provide clues that predict the differences in centrosome aberration frequency and thus genomic instability post exposure. We assessed the activation of key mediators that are thought to sustain multi-protein interactions to provide positive signaling feedback (γH2AX), transducers that phosphorylate check point kinases (ATM, ATR) and effectors that determine cell fate choices, such as undergoing cell-cycle arrest or apoptosis in response to radiation damage (P53, MDM2, P21, Chk1, Chk2). We chose a 24 h and 72 h time point after exposure to understand how persistent DNA damage (either unrepaired or mis repaired lesions at these time points) would impact the expression and activation (phosphorylation) of key proteins

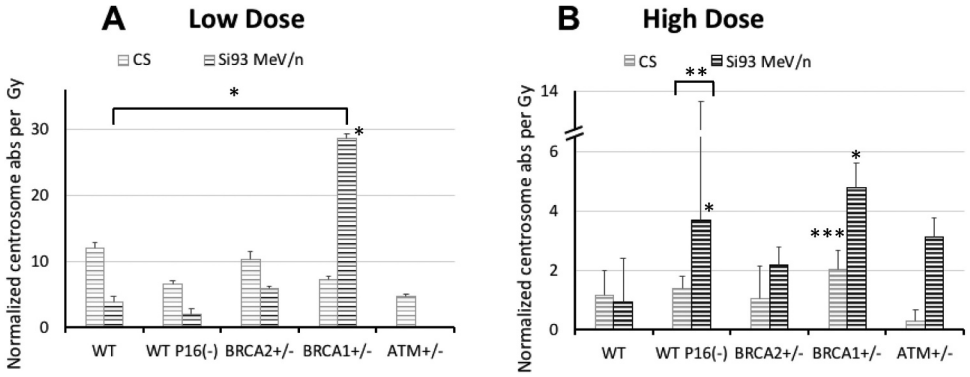

Fig. 1. Centrosome aberrations are higher in genetic variants following high dose exposure to Si 93 MeV/u

Five HMEC strains derived from individuals of various genetic backgrounds were exposed to a single low dose (LD) and a high dose (HD) of two types of radiation, namely Cs and Si 93 MeV/u. These include: (1) a 184 strain used as a wild type (WT) reference, (2) a WT P16(-) strain wherein p16 is silenced, (3) a BRCA2+/− strain (4) a BRCA1+/− and (5) an ATM +/− strain. Slides were fixed 3 days post exposure and centrosomes were visualized by indirect immunofluorescence microscopy using an anti-pericentrin antibody. The frequency of aberrant centrosomes were normalized to sham irradiated controls and aberrations generated by low dose (Fig. 1A) and high dose (Fig. 1B) were graphed per unit dose. As the normalized data was graphed per unit dose (Gy), error bars were not plotted on the graphs. Cs and Si exposed samples were distinguished by grey and black lines respectively. Data is based on two independent experiments with error bars representing SD. Notations; $*=p < 0.05$, $**=p < 0.01$, $***=p < 0.001$ alone were used to indicate changes relative to sham irradiated controls, and horizontal bars with notations "*" were used to indicate significance of pair-wise comparisons.

involved in cell cycle regulation that in turn deregulate centrosome numbers. Due to the observed increase in centrosome aberrations following a high dose of Si 93 MeV/u exposure in Fig. 1, we centered our analysis on checkpoint protein responses following high dose exposures. Our results revealed that with Cs exposure, both total protein levels of ATR, MDM2 and p21 and phosphorylated levels of Chk1 (Ser345), Chk2 (Thr68), H2AX (Ser139) and p53 (Ser15) were very similar in the WT and WTP16(-) strains (Fig. 3A and B). However, following exposure to Si 93 MeV/u most of these nodes were elevated in and WTP16(-) culture as compared to the normal pre-stasis strain (Fig. 3C and D). P21 was the only target that showed no change in expression with or without P16 expression. 24 h post exposure, pP53 showed the greatest difference between the WT strain and its P16(-) derivative (Fig. 3C), but at 72 h, pChk2, pChk1, ATR and γH2AX showed a higher increase in the WTP16(-) culture in comparison to WT (Fig. 3D). It is notable that in the p16 shRNA post-stasis culture, the levels of all seven of these proteins was higher post Si 93 ion exposure as compared to cesium both at 24 h as well as 72 h post exposure. Comparing changes in protein and phospho-protein expression to centrosome changes (Fig. 3E) an analogous pattern is observed with the p16 silenced WT sample showing a greater significant effect ($p < 0.05$), post exposure to Si 93 MeV/u. Despite the observed similarity in patterns of centrosome aberration frequency and activation of the seven DNA damage response markers, a significant correlation between end points was not observed.

Similar to what was observed in the p16(-) post-stasis strain, the BRCA1+/− strain showed no increase with Cs exposure (Fig. 4A) and a transient elevation in all of these protein targets at 24 h (Fig. 4C). In addition to p53, a large variation between WT and BRCA1+/− strains was noted for γH2AX, ATR and pChk2. The majority of these nodes continue to remain elevated in the BRCA1+/− strain at 72 h post Si 93 exposure, both in comparison to WT (Fig. 4D) and to cesium exposed samples (Fig. 4B vs 4D). This increase appears to mimic the increase in centrosome aberrations noted with Si93 in the BRCA1+/− strain ($p < 0.05$) (Fig. 4E), though the statistical correlations weren't significant. Notably, differences between the WT and BRCA1+/− strains appear less than what was observed between WT pre-stasis and p16-post-stasis culture.

Following cesium exposure there is almost no difference between WT and BRCA2+/− in the various protein and phospho-protein expressions (Fig. 5A and B). However, with Si93 exposure the levels of all of these proteins are much higher in the BRCA2 + /- carrier in comparison to WT at 24 h post exposure (Fig. 5C), with γH2AX, pChk1, pChk2 and p53 showing the largest difference between WT and the BRCA2 + /- variant. Similar to the BRCA1+/− strain, the BRCA2+/− strain shows an increase in protein expression levels at 72 h (Fig. 5D) that parallels the increase in centrosome aberrations noted in the BRCA2+/− sample when comparing to Cs and Si exposure results (Fig. 5E). With the exception of p21, BRCA2+/− shows a larger increase in levels of proteins relative to WT. Our results indicate increased levels of ATR, phospho-p53, γH2AX, p21, MDM2, pChk1 and pChk2 with high dose exposure to Si93 in both of the BRCA variant cell strains with high dose exposure. This activation continues to persist at longer times (72 h) post damage. Unlike high dose exposure, the two genetic variants BRCA1+/− and BRCA2+/−, as well as the WT p16-silenced culture, exhibit a lower level of expression at 72 h post exposure as compared to the WT pre-stasis strain following low dose exposure to Cs that results in more simple lesions (Appendix Figs. 2B, 3B and 4B). These findings appear to parallel the lower level of centrosome aberrations with these exposures. Interestingly, while the levels of expression are higher in all of the genetic variants at 24 h post Si 93 exposure (Appendix Figs. 2C, 3C and 4C), we noted a different pattern at 72 h.

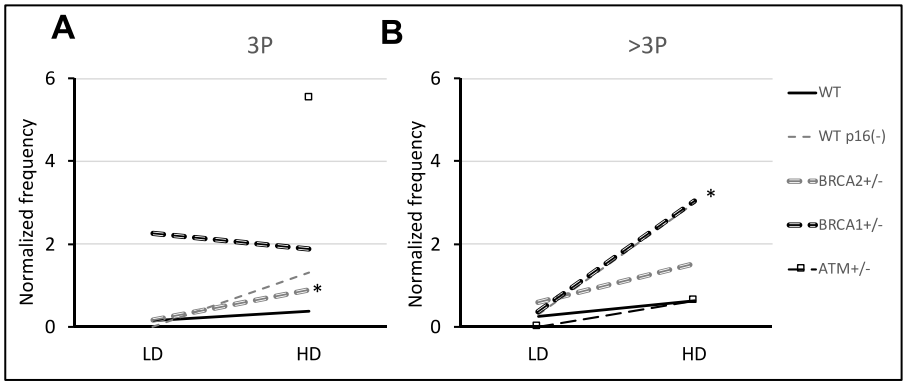

Fig. 2. The number of aberrant centrosomes per cell generated by complex lesions is dependent on the genetic background.

Cells with centrosome aberrations generated by high dose exposure to Si 93 MeV/u were further stratified into two populations, one with 3 centrosomes (3P = 3 pericentrin foci) and those that had 4 or more centrosomes (> 3P pericentrin foci). The fraction of cells with 3P and > 3P were graphed relative to control. The dose effect on the change in 3P (A) and > 3P (B) population relative to the un-irradiated control is shown for all strains. Data for the ATM+/− HD sample is represented by a square marker. ($*=p < 0.05$, $**=p < 0.01$, $***=p < 0.001$).

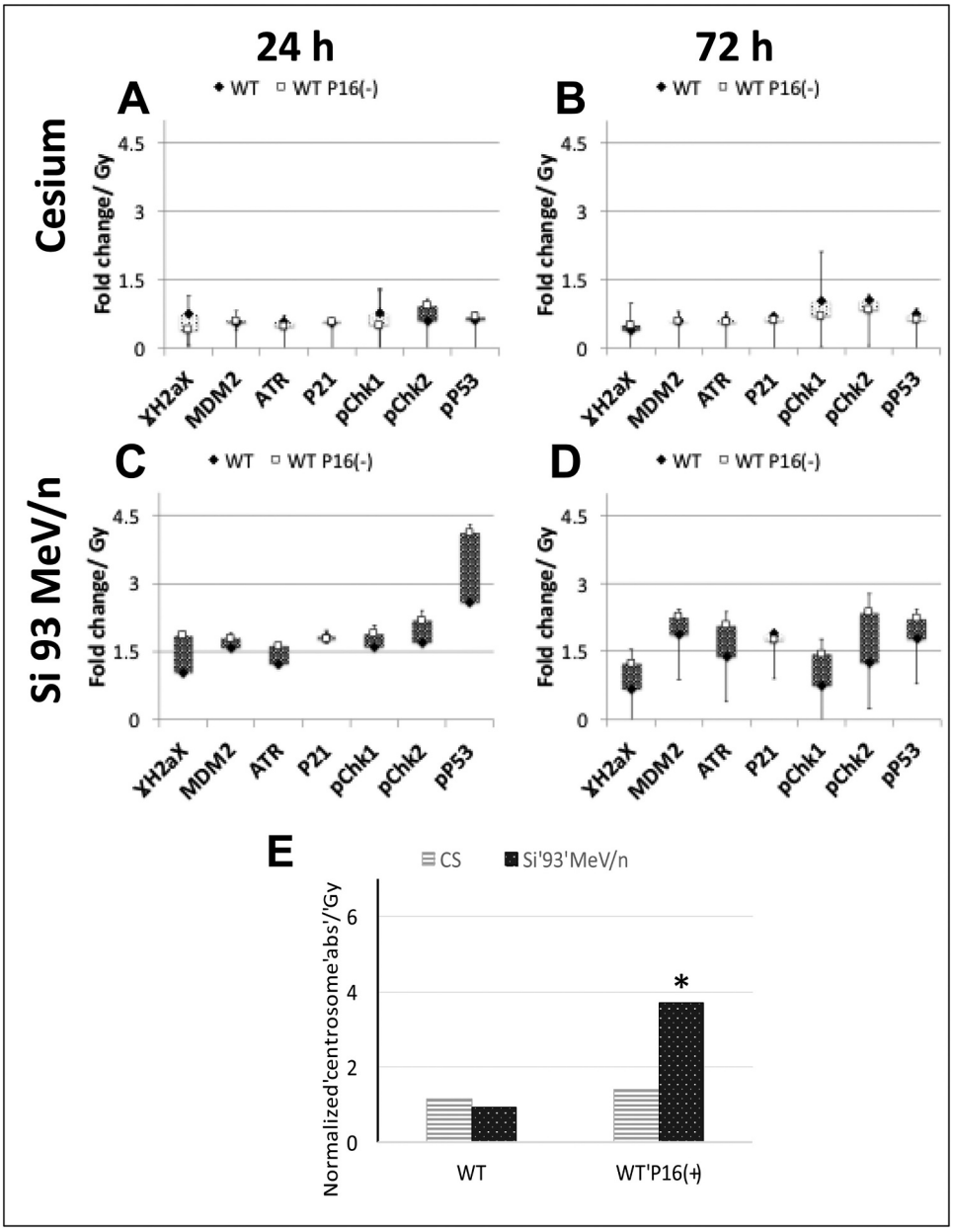

Fig. 3. Comparison of DNA response multiplex analysis in WT and WT p16 silenced derivative post radiation exposure.
WT 184D HMEC with and without p16 silencing were exposed to a low and a high dose of either Cs or Si93 MeV/u. Cell lysates at 24 h and 72 h post exposure were processed using the MILLIPLEX® MAP 7-plex DNA Damage/Genotoxicity Magnetic Bead kit (EMD Millipore Inc, MA) to detect MFI in phosphorylated Chk1 (Ser345), Chk2 (Thr68), H2AX (Ser139) and p53 (Ser15) as well as total protein levels of ATR, MDM2 and p21 in cell lysates using the Luminex system. The average MFI per unit dose for high dose exposed samples relative to control and standard deviation of two independent experiments were graphed. Levels of the various targets in wild type (black diamond marker) marker were compared to the genetic variant (white square marker), the p16 silenced strain (Fig. 3-A, B, C, D). Up/down bars were used to highlight trends in the genetic variants relative to wild type. Levels higher than wild type are represented by dark shaded bars and lower than wild type are represented by white shaded bars. Expression of targets between strains were compared to the centrosome aberration frequencies in Fig. 3E. (*=$p < 0.05$, **=$p < 0.01$, ***=$p < 0.001$).

Although the expression levels in the p16 silenced culture were similar and slightly lower than the WT pre-stasis HMEC (Appendix Fig. 2D), the levels in BRCA1 +/− and BRCA2 +/− were higher (Appendix Figs. 3D and 4D), which reflects the pattern of centrosome aberrations in each of these strains (Appendix Figs. 2E, 3E and 4E), relative to WT.

Although centrosome aberrations at 72 h revealed a similar pattern of increase with protein and phospho-protein expression for each of the variant strains, overall a significant correlation between centrosome aberration frequencies and any of the seven DNA damage response markers was not observed. However, not surprisingly, we did note a strong correlation amongst some of the DNA repair nodes, which confirmed their documented interaction in DNA damage response. ATR levels showed a significant correlation with pChk1($p < 0.05$), γH2AX ($p < 0.05$) and MDM2($p < 0.001$); pChk1 levels showed significant correlation with pChk2 ($p < 0.05$), γH2AX($p < 0.05$), p53 ($p < 0.05$) and MDM2 ($p < 0.005$), pChk2 levels showed a strong correlation with MDM2 ($p < 0.05$) and pP53($p < 0.001$) and γH2AX levels showed a significant correlation with phospho-p53 ($p < 0.05$) and MDM2 ($p < 0.05$).

3.4. Long-term increase in centrosome aberration frequencies post exposure to Si 93 Mev/u is independent of genetic background

Given levels of several of the nodes involved in check point regulation show higher levels in the genetic variant strains and the p16 silenced WT derivative as compared to wild type at 72 h, we next examined whether this would have an impact on the frequency of centrosome aberrations after a couple of division cycles post exposure. To assess the temporal dependence of centrosome induction, we scored centrosome aberrations 9 days post Cs and Si 93 MeV/u exposure. Our data revealed that the frequency of centrosome aberrations increased notably for all of the heterozygote strains with Si 93 MeV/u as compared to Cs exposed samples (Fig. 6). Unlike the results observed at Day 3, this increase was noted with both low and high doses (Fig. 6A and B) with the WTp16 knockdown and BRCA2 +/− showing significant increases relative to control ($p < 0.001$). The frequency of centrosome aberrations in the WT cell strain as compared to its genetically silenced P16(-) derivative revealed that aberrations were relatively higher in the pre-stasis Vs post-stasis culture following both high and low dose

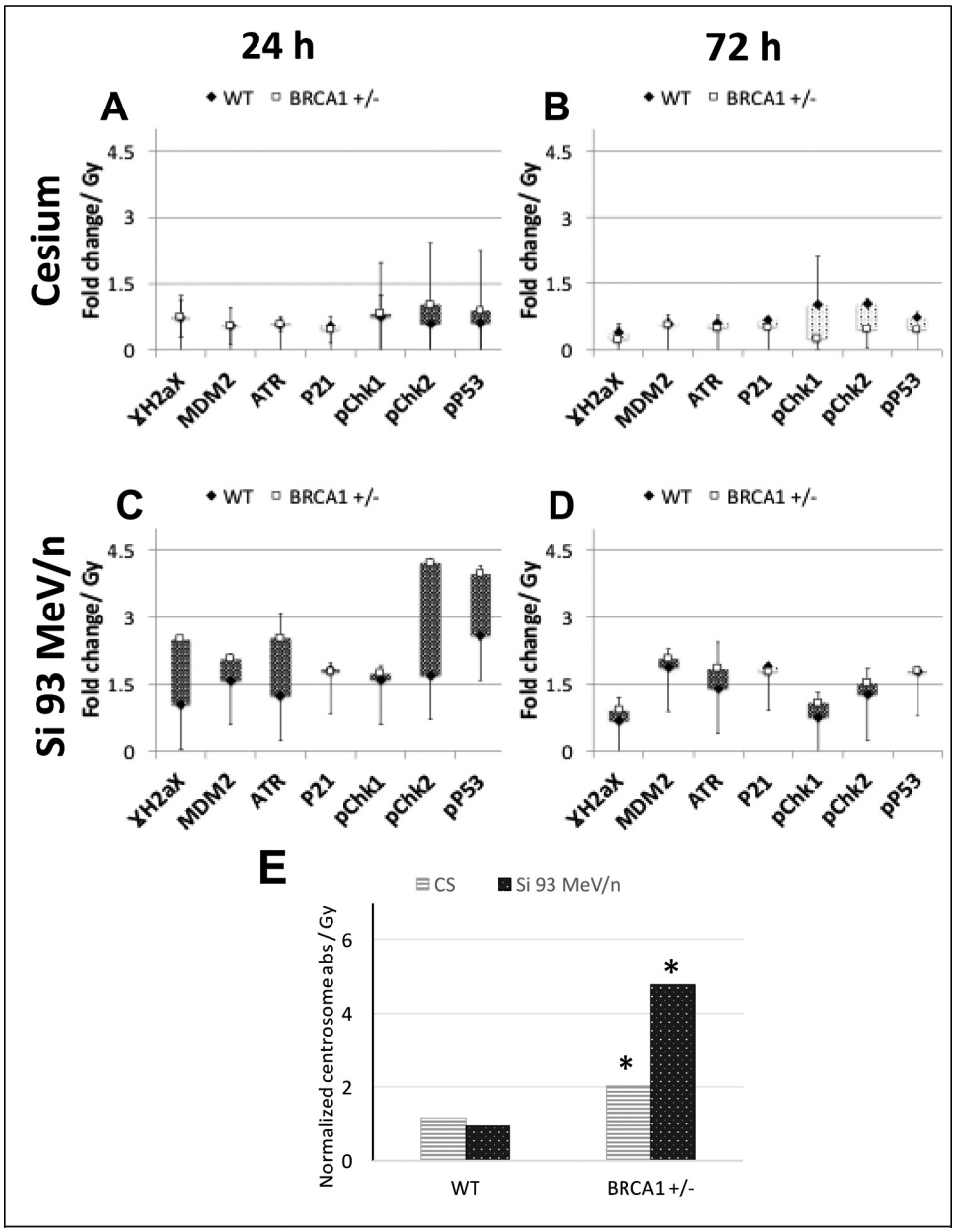

Fig. 4. Expression and activation of DNA damage cell cycle check point regulation proteins in WT and BRCA1 +/− strain

Strains were exposed to radiation and processed similar to Fig. 3. The average MFI per unit dose for high dose exposed samples relative to control and standard deviation of two independent experiments were graphed. The expression and activation of the multiplexed proteins were assayed between WT and BRCA1 +/− with cesium exposure (Fig 4A and B) and Si 93 exposure (Fig 4C and 4D). The pattern of expression was compared to centrosome aberration frequencies at 72 h post exposure (Fig 4E). (*=$p < 0.05$, **=$p < 0.01$, ***=$p < 0.001$).

exposure to Si 93 MeV/u. Centrosome aberration levels were higher at Day 9 (Fig. 6) as compared to Day 3 (Fig. 1) for most of the cell strains, with the exception of the p16 silenced and ATM +/− strains where levels were lower. These results suggest that the long term impact of complex lesions on genomic instability is independent of genetic background.

3.5. Centrosome aberrations in genetic variants are dependent on radiation type

We next posed the question whether centrosome aberration frequency could be modified by the nature of complex lesion inducing exposure. To address this query, we examined centrosome aberrations in WT, BRCA2 +/−, BRCA1 +/− and ATM +/− strains 9 days post exposure to a high dose of Ti300 MeV/u (0.5 Gy) ion, a radiation quality that has a higher energy than Si 93, and higher degree of energy deposited per unit distance in the cell (a higher Linear energy transfer, LET). Unlike Si93 MeV/u, where the BRCA2 +/− strain shows the highest level of aberrations as compared to the BRCA1 +/− and ATM +/− strains, with Ti300 MeV/u exposure we see an inverse pattern with the ATM +/− strain exhibiting the highest level of aberrations ($p < 0.01$) (Fig. 7).

3.6. Validating the linear relationship between age and centrosome aberration based on lesion complexity

As radiation quality effects were difficult to discern when comparing genetic variants, we attempted to tease out the difference in effectiveness of Si 93 MeV/u and Ti 300 MeV/u using a subset of the aged cohort of cell strains (2 young, 2 middle aged and 2 older strains) previously shown to exhibit an age effect with high dose Ti 300 MeV/u exposure (Sridharan et al., 2017). Centrosome aberrations were assessed 9 days post exposure. Our results revealed a similar age dependent increase with exposure to Si 93 MeV/u with a steeper slope than Ti 300 MeV/u (Fig. 8). These results demonstrated that the lower energy ions, such as Si 93 MeV/u are more effective in generating centrosome aberrations as compared to higher energies like Ti 300 MeV/u and that age impacts the levels of aberrations.

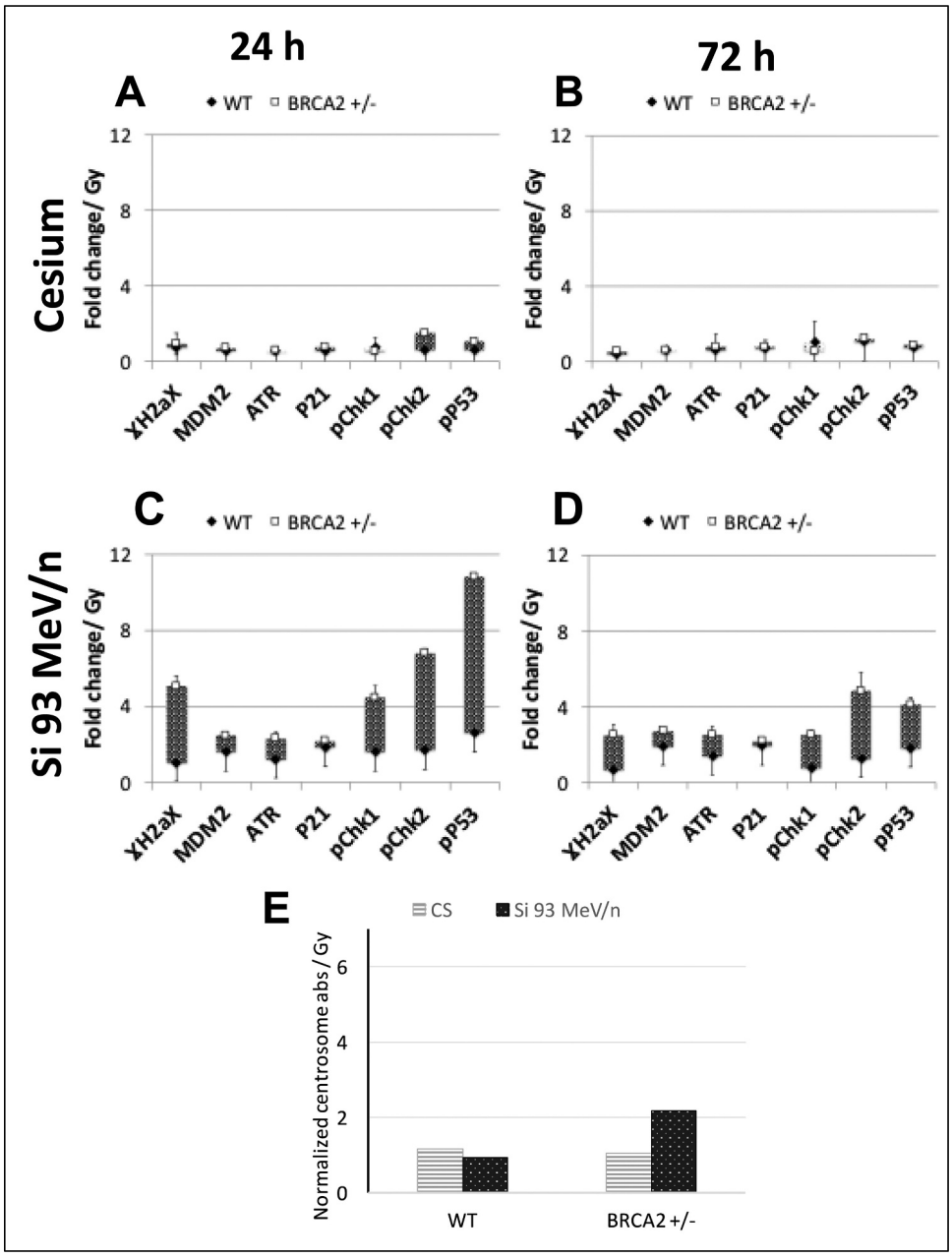

Fig. 5. Expression and activation of DNA damage cell cycle check point regulation proteins in WT and BRCA2 +/− strains

The BRCA2 +/− strain was processed similar to p16(-) strain and the BRCA1 +/− strains (Fig. 3 and 4) and compared to wild type. The average MFI per unit dose for high dose exposed samples relative to control and standard deviation of two independent experiments were graphed. The expression and activation of the multiplexed proteins were assayed between WT and BRCA2 +/− with cesium exposure (Fig. 5A and B) and Si 93 exposure (Fig. 5C and 4D). The pattern of expression was compared to centrosome aberration frequencies at 72 h post exposure (Fig. 5E). (* = $p < 0.05$, ** = $p < 0.01$, *** = $p < 0.001$).

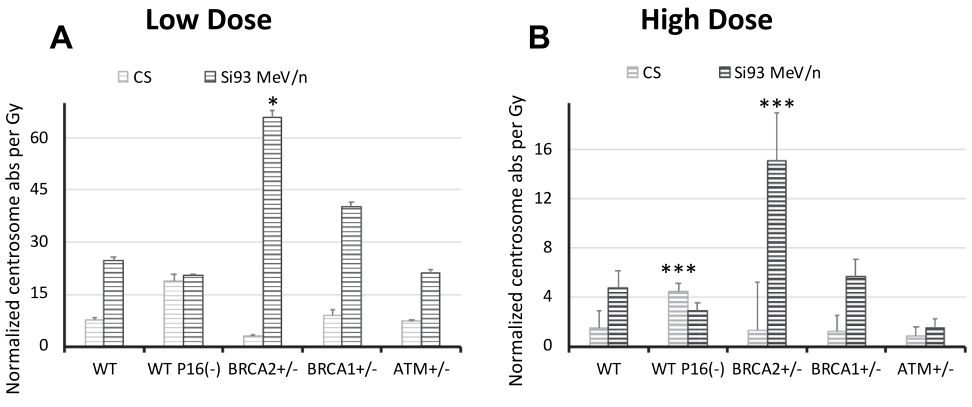

Fig. 6. Centrosome aberrations generated by complex damages at 9 days post exposure are independent of genetic background.

Wild type and genetic variant strains were exposed to a high and low dose of Cs and Si and cultured for 9 days prior to fixation. Slides were stained with anti-pericentrin antibody and centrosome aberrations were scored similar to the Day 3 samples. The frequency of aberrant centrosomes generated by low dose exposure (Fig. 6A) and high dose exposure (Fig. 6B) were normalized to sham radiated controls. Cs and Si exposed samples were distinguished by grey and black lines. Data is based on two independent experiments with error bars representing SD. (* = $p < 0.05$, ** = $p < 0.01$, *** = $p < 0.001$).

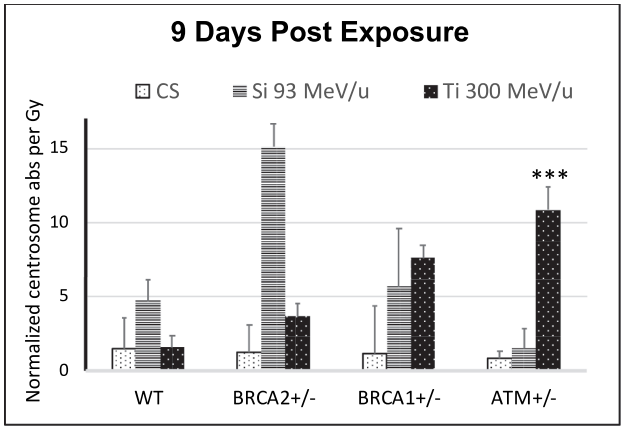

Fig. 7. Lower energy exposures are more biologically effective in generating centrosome aberrations.
WT, BRCA1 + / −, BRCA2 + / − and ATM + / − strains were exposed to high doses of Cs, Si 93 and Ti 300 MeV/u and processed 9 days post exposure for immunofluorescent microscopy. The percentage of aberrant cells in each strain was plotted relative to the unexposed population. Data is based on 2 independent experiments for Cs, Si93 and Ti300. The normalized frequency of cells with supernumerary (> 2N) centrosomes was graphed per unit dose.

4. Discussion

Our main goal was to test whether genetic variation confers increased risk for the development of cancer predisposing phenotypes post exposure to HZE radiation. We chose to study centrosome aberrations as our surrogate end point of cancer risk, as it has been well documented that aberrations in centrosome number can disrupt tissue architecture and genomic instability; the two main hallmarks of carcinogenesis (Nigg, 2006; Rivera-Rivera & Saavedra, 2016). We and others have also shown that centrosome defects increase with simple and complex damage (Sato et al., 1983; Sudo et al., 2008, Sridharan et al., 2017) and can sensitively differentiate between radiation and age dependent effects (Sridharan et al., 2017). However, the influence of individual genetics in eliciting centrosome defects with exposure to complex damages is not well-understood.

In this study, we have shown that HMEC strains derived from individuals who are heterozygote carriers of ATM, BRCA1, BRCA2 mutations have an increased frequency of centrosome aberrations following exposure to Si 93 MeV/u relative to a WT non-carrier individual. There is overwhelming evidence that indicate that complex lesions that result from the unique track structure of high LET, result in persistent damage that lasts days to weeks post exposure. We have also shown that exposure to Si93 MeV/u results in a higher degree of persistent signaling of various repair response proteins, 24 h post exposure in comparison to low LET radiation (Sridharan et al., 2015). Thus it is tempting to speculate that the increase in aberrations with high LET is directly due to sensitivity to complex damages in these strains. Future work using live cell microscopy to combine these endpoints would be useful to validate this relationship. Centrosome over-duplication during prolonged cell cycle arrest, failure of cell division post centrosome duplication and centrosome fragmentation from radiation exposure (Godinho and Pellman, 2014; Nigg, 2006) are potential theories that could explain the increase in centrosome numbers. We have shown a notable increase in the activation of proteins/phospho-proteins involved in DNA damage checkpoint activation such as γH2AX, ATR, pChk1, pChk2 and p53 in the heterozygote strains and the p16 silenced culture exposed to high doses of Si 93MeV/u. While differences between normal and Het strains, and correlations between centrosome aberrations and DNA damage response markers show similar patterns, the results are not statistically significant. A higher n in future experiments would help in addressing the significance of the observed patterns. Though the trends observed are not significant, our results suggest important correlations that may have mechanistic implications. Nevertheless, these data provide indirect evidence to suggest that centrosome duplication during prolonged checkpoint arrest elicited by complex lesions is a causal factor for increased aberrations in these strains. However, additional studies directly examining cell cycle arrest would be essential to confirm this finding.

Our study has revealed that following a high dose of radiation exposure haploinsufficiency of BRCA1 produces a much higher frequency of centrosome aberrations than that observed in the ATM + / − or BRCA2 + / − carriers. Both ATM and BRCA1 are known to have important roles in regulating activation of cell cycle checkpoints and inducing arrest in response to DSB damage. BRCA1 not only regulates G1/S, S, G2/M transition but also regulates the spindle checkpoint that is critical for chromosome segregation (Deng, 2006; Wang et al., 2004). In addition, several lines of evidence point to a key role of BRCA1 in centrosome duplication. This multifaceted protein has been shown to interact with gamma tubulin, a well-known component of the centrosome, several proteins (p53, BRCA2, Rb, CDK2-CyclinA and CDK2-cyclin E) that play key roles in centrosome duplication (Fukasawa et al., 1996; Hinchcliffe et al., 1999; Hollander et al., 1999; Hsu and White, 1998; Mantel et al., 1999; Meraldi and Nigg, 2002; Meraldi et al., 1999; Tutt et al., 1999) and regulates transactivation of specific genes involved in centrosome duplication, such as p21 and Gadd45 (Harkin et al., 1999; Somasundaram et al., 1997). The nature of post translational modifications (hypo- versus hyper-phosphorylation) of BRCA1 is also thought to provide a switch controlling centrosome duplication (Deng, 2002). Furthermore, studies have shown that in addition to DSBs, BRCA1 is involved in the repair of non-DSB clustered lesions,

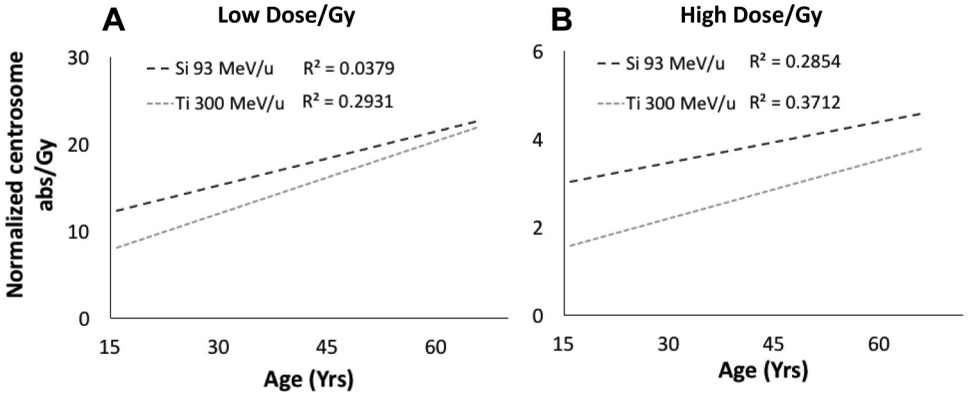

Fig. 8. Validation of an age effect on centrosome aberration levels with exposure to Si 93 MeV/u.
Six HMEC strains derived from individuals of various ages (2 young, 2 middle and 2 old) were exposed to a low dose 0.05 Gy (LD) and high dose 0.5 Gy (HD) of two types of ions that introduce complex damages; namely Ti 300 MeV/u and Si 93 MeV/u. Cells were processed 9 days post exposure and the percentage of aberrant cells (> 2P) in each strain was plotted relative to the unexposed population. Data is based on 4 independent experiments for high dose Ti 300 MeV/u and 2 independent experiments for Si 93 MeV/u. The frequency of cells with supernumerary (> 2N) centrosomes was graphed against age of the individual from which the strain was derived. Regression analysis was used to model the relationship with age. The effects of lesion complexity on the relationship with age is graphed for low (C) and high dose (D). Si 93 and Ti 300 MeV/u regression curves were distinguished using black and grey dotted lines, respectively.

oxidative lesions [Hair, 2010], and enhancing the Base excision repair pathway [Saha, 2010]; functions that are thought to be supported by its multifaceted role as a coordinator various DNA repair proteins as ex-pounded by the BASC model [Wang, 2000]. Cumulatively, its combined functions in regulation of centrosome duplication, check point activa-tion and damage of DSB and non-DSB lesions in clustered damages, could explain the higher frequency of aberrations in BRCA1+/− car-riers as opposed to the BRCA2+/− and ATM+/− strains. With low doses of Si93 MeV/u exposure, even when only ~25% of the cells are directly damaged by exposure, BRCA1+/− cells still exhibit higher centrosome aberration frequencies. This increased genomic instability in the BRCA1+/− strain at low doses as compared to BRCA2+/− and ATM+/− heterozygote strains, suggests that BRCA1 carriers are ex-quisitely sensitive to the non-targeted effects of Si ion exposure.

ATM acts a sensor of DNA damage and similar to BRCA1, ATM activation can arrest cells in all three phases (G1, S or G2) of the cell cycle by phosphorylation of different targets p53, cAbl, Chk1, Chk2 etc (Baskaran et al., 1997; Canman et al., 1998; Khanna et al., 1998; Shafman et al., 1997). ATM also localizes to the centrosome and interacts with gamma tubulin, P21 and P53 in regulating centrosome biogenesis (Shen et al., 2006), all of which support the increased centrosome aberration in the ATM+/− strain relative to WT. Unlike BRCA1 and ATM, a direct role in regulating cell cycle checkpoints has not been established for BRCA2. Although BRCA2 loss of function mutations appear to suggest defects in checkpoint control (Daniels et al., 2004), disruption of BRCA2 does not have a marked effect on cell cycle checkpoint control (Patel et al., 1998), which could explain the lower frequency of centrosome aberrations in BRCA2 in comparison to BRCA1 and ATM heterozygote strains at early times following exposure to high doses of Si 93 MeV/u. Interestingly, the centrosome aberration frequency is lower in both the BRCA1 and ATM heterozygote strains in comparison to BRCA2+/−, 9 days post Si 93 MeV/u exposure. One likely possibility for this finding is that severe genomic instability in these BRCA1 and ATM strains at early time points targets these cells for apoptosis. Thus the BRCA2 heterozygote strain with a better proliferative advantage is perceived more genomically unstable 9 days post exposure.

Given the common loss of p16 protein expression observed during breast carcinogenesis in vivo, including the finding of rare p16- cells within the breast tissue of some normal individuals, we examined a wild type normal pre-stasis cell strain and its p16 silenced post-stasis derivative to test whether overcoming the stasis senescence barrier could alter surrogate phenotypes associated with carcinogenesis. It has been previously shown that transduction of p16 shRNA significantly decreased p16 expression in this cell strain without altering the normal karyotype (Garbe et al., 2014; Lee et al., 2015). Our studies indicate that centrosome aberrations generated in the background of loss of p16 expression are higher following complex damages as compared to exposures causing more simple lesions. In fact, higher doses showed significantly more aberrations per unit dose than low dose exposures. Studies by McDermott et al have shown that loss of p16 can generate supernumerary centrosomes through centriole pair splitting that potentiates genomic instability and results in aneuploidy by generating multipolar mitosis (McDermott et al., 2006). The ability to amplify centrosome numbers appears to be through its regulation of cdk2 activity, which is essential for initiation of normal centrosome duplication (Lacey et al., 1999; Matsumoto et al., 1999; Meraldi et al., 1999). Furthermore, the increase in centrosome numbers associated with p16 loss appears to be coupled with conditions that inhibit DNA replication (McDermott et al., 2006). Thus, previous work in combination with our own supports the possibility that complex damage exposures may stall DNA replication and cause more centrosome aberrations in strains with a p16 deficient background.

Its well-recognized that individual response to varied exposures can differ greatly. Our studies have revealed that differences in age, the complexity of lesion, and the genetic background of the exposed individual may all play a role. Although pairwise comparison of doses, and radiation quality within each cell line showed few significant hits, analysis of trends comparing the variant cell lines as a group to wild type, revealed significant differences in radiation quality (Cs Vs Si93, p value = 0.008), and cell type differences ($p = 0.05$) in the Day3 high dosed exposed samples; and significant dose effects in D3 Cs ($p = 0.009$), D9 Cs ($p = 0.05$) and Day9 Si 93 MeV/u ($p = 0.02$). We have also observed that the radiation quality of the exposure plays a role in the differences observed in the context of age. This finding is revealed by the lower energy ion, Si 93 MeV/u showing more effectiveness in generating centrosome aberrations as compared to Ti 300 MeV/u, in the aged cohort. Despite similarities in Z^2/β^2 values of these two radiation qualities, the inherent track structure is different for these two ions. Si 93 ions have a lower LET (150 keV/μm) and smaller track width (525 μm), but has more hits in the cell core (0.84) and more hits in the penumbra (6.6) in comparison to Ti 300 ions which have a higher LET (171 keV/μm) and larger track width (3371 μm), but has fewer hits in the cell core (0.73) and fewer hits in the penumbra (5.5.). This increased deposition of hits close to the track, could account for the higher effectiveness of Si93 in comparison to Ti 300 MeV/u. These results parallel our previous data that show higher effectiveness of lower energy ions in generating both initial and persistent damage post exposure to complex lesions (Sridharan et al., 2015). Although both radiation qualities show a similar age dependent increase, Si ions show a steeper response slope in the aged cohort and validate our previous finding of age-related increase in centrosome aberration with lesion complexity.

In summary, efforts to understand radiosensitivity of genetic variants such as ATM, BRCA1 and BRCA2 heterozygotes and their relationship to breast cancer susceptibility is a topic that has been fraught with significant controversy with some studies showing enhanced radiosensitivity in heterozygotes in comparison to the normal population (Abbott et al., 1999; Paterson et al., 1979; Weeks et al., 1991) while others suggesting that cellular radiosensitivity is not altered in carriers (Weissberg et al., 1998). Lack of clarity on the susceptibility conferred by genetic variation poses barriers in estimating individualized cancer risk from radiation exposures, especially those that generate clustered lesions. Our pilot study has provided promising results which indicate that in addition to radiation quality, dose and complexity of the DNA lesion generated by lower energy ions, genetic background appears to have a significant impact on genomic instability at early time points post high LET exposure. This increase in centrosome aberration is likely caused by persistent damage and prolonged check point activation. A more expansive study including more strains for each genetic variant is essential to assign weights for genetic variation for use in cancer risk modeling from HZE exposure.

Author contributions statement

J.M.P and D.M.S designed and planned the experiments, J.M.P., D.M.S and S.E conducted the experiments, D.M.S., C.W., and S.E., analyzed the results, M.A.L and M.S generated and provided cell strains at P2 and consulted on experimental design. D.M.S. wrote the manuscript. All authors reviewed the manuscript.

Acknowledgements

We thank our research assistants Mary Whalen, Wade Wilson and Jonathan Lee for generating cell stocks and undergraduate volunteers, Jessica Chen and Roshni Narasimhan for their assistance with microscopy and centrosome scoring. Our thanks to Drs. Sasha Langley and Ben Brown at LBL for statistical analysis consultation. We also thank the physics and medical teams at Brookhaven National Laboratory for supporting the high LET experiments. Lastly, we thank Dr. Matthew Coleman, Nicholas Hum, and Salustra Urbin at Lawrence Livermore National Laboratory for supporting the cesium experiments.

Funding statement/Grant sponsors

NASA grants NNJ13HA96I and NNJ12HD071 awarded to JMP funded this study. Funds from DOE Laboratory Directed Research and Development, contract no DE-AC02-05CH11231, NIH R01AG040081 and DOD BC141351 awarded to MAL funded the development of the strains used from the HMEC Aging Resource.

Conflict of interest

The authors declare no competing financial interests.

Supplementary materials

Supplementary material associated with this article can be found, in the online version, at doi:10.1016/j.lssr.2018.10.002.

References

Abbott, D.W., Thompson, ME, Robinson-Benion, C, Tomlinson, G, Jensen, RA, Holt, JT., 1999. BRCA1 expression restores radiation resistance in BRCA1-defective cancer cells through enhancement of transcription-coupled DNA repair. J. Biol. Chem. 274 (26), 18808–18812.

Ahmed, M., Rahman, N., 2006. ATM and breast cancer susceptibility. Oncogene 25 (43), 5906–5911.

Aparicio, T., Baer, R, Gautier, J, 2014. DNA double-strand break repair pathway choice and cancer. DNA Repair 19, 169–175.

Baskaran, R., Wood, LD, Whitaker, LL, Canman, CE, Morgan, SE, Xu, Y, Wang, JY, 1997. Ataxia telangiectasia mutant protein activates c-Abl tyrosine kinase in response to ionizing radiation. Nature 387 (6632), 516–519.

Brenner, A.J., Paldugu, A., Wang, H., Olopade, O.I., Dreyling, M.H., Aldaz, C.M., 1996. Preferential loss of expression of p16(INK4a) rather than p19(ARF) in breast cancer. Clin. Cancer Res. 2 (12), 1993–1998.

Brenner, A.J., Stampfer, M.R., Aldaz, C.M., 1998. Increased p16 expression with first senescence arrest in human mammary epithelial cells and extended growth capacity with p16 inactivation. Oncogene 17 (2), 199–205.

Broeks, A., Urbanus, J.H., Floore, A.N., Dahler, E.C., Klijn, J.G., Rutgers, E.J., van't Veer, L.J., 2000. ATM-heterozygous germline mutations contribute to breast cancer-susceptibility. Am. J. Hum. Genet. 66 (2), 494–500.

Canman, C.E., Lim, D.S., Cimprich, K.A., Taya, Y., Tamai, K., Sakaguchi, K., Siliciano, J.D., 1998. Activation of the ATM kinase by ionizing radiation and phosphorylation of p53. Science 281 (5383), 1677–1679.

Daniels, M.J., Wang, Y., Lee, M., Venkitaraman, A.R., 2004. Abnormal cytokinesis in cells deficient in the breast cancer susceptibility protein BRCA2. Science 306 (5697), 876–879.

Davies, A.A., Masson, J.Y., Mcllwrath, M.J., Stasiak, A.Z., Stasiak, A., Venkitaraman, A.R., West, S.C., 2001. Role of BRCA2 in Control of the RAD51 Recombination and DNA Repair Protein. Mol. Cell 7 (2), 273–282.

Deng, C.X., 2002. Roles of BRCA1 in centrosome duplication. Oncogene 21 (40), 6222–6227.

Deng, C.X., 2006. BRCA1: Cell cycle checkpoint, genetic instability, DNA damage response and cancer evolution. Nucl. Acids Res. 34 (5), 1416–1426.

Falck, J., Mailand, N., Syljuasen, R.G., Bartek, J., Lukas, J., 2001. The ATM-Chk2-Cdc25A checkpoint pathway guards against radioresistant DNA synthesis. Nature 410 (6830), 842–847.

Fukasawa, K., Choi, T., Kuriyama, R., Rulong, S., Vande Woude, G.F., 1996. Abnormal centrosome amplification in the absence of p53. Science 271 (5256), 1744–1747.

Garbe, J.C., Bhattacharya, S., Merchant, B., Bassett, E., Swisshelm, K., Feiler, H.S., Stampfer, M.R., 2009. Molecular distinctions between stasis and telomere attrition senescence barriers shown by long-term culture of normal human mammary epithelial cells. Cancer Res. 69 (19), 7557–7568.

Garbe, J.C., Holst, C.R., Bassett, E., Tlsty, T., Stampfer, M.R., 2007. Inactivation of p53 function in cultured human mammary epithelial cells turns the telomere-length dependent senescence barrier from agonescence into crisis. Cell Cycle 6 (15), 1927–1936.

Garbe, J.C., Vrba, L, Sputova, K, Fuchs, L, Novak, P, Brothman, AR, Jackson, M, Chin, K, LaBarge, MA, Watts, G, Futscher, BW, Stampfer, MR., 2014. Immortalization of normal human mammary epithelial cells in two steps by direct targeting of senescence barriers does not require gross genomic alterations. Cell Cycle 13 (21), 3423–3435.

Godinho, S.A., Pellman, D., 2014. Causes and consequences of centrosome abnormalities in cancer. Philos. Trans. R. Soc. Lond. B Biol. Sci. 369, 1650.

Harkin, D.P., Bean, JM, Miklos, D, Song, YH, Truong, VB, Englert, C, Christians, FC, Ellisen, LW, Maheswaran, S, Oliner, JD, Haber, DA., 1999. Induction of GADD45 and JNK/SAPK-dependent apoptosis following inducible expression of BRCA1. Cell 97 (5), 575–586.

Hinchcliffe, E.H., Li, C, Thompson, EA, Maller, JL, Sluder, G., 1999. Requirement of Cdk2-cyclin E activity for repeated centrosome reproduction in Xenopus egg extracts. Science 283 (5403), 851–854.

Hollander, M.C., Sheikh, MS, Bulavin, DV, Lundgren, K, Augeri-Henmueller, L, Shehee, R, Molinaro, TA, Kim, KE, Tolosa, E, Ashwell, JD, Rosenberg, MP, Zhan, Q, Fernández-Salguero, PM, Morgan, WF, Deng, CX, Jr, FornaceAJ, 1999. Genomic instability in Gadd45a-deficient mice. Nat. Genet. 23 (2), 176–184.

Holst, C.R., Nuovo, GJ, Esteller, M, Chew, K, Baylin, SB, Herman, JG, Tlsty, TD., 2003. Methylation of p16INK4a promoters occurs in vivo in histologically normal human mammary epithelia. Cancer Res. 63 (7), 1596–1601.

Hsu, L.C., White, R.L., 1998. BRCA1 is associated with the centrosome during mitosis. Proc. Natl. Acad. Sci. USA 95 (22), 12983–12988.

Karami, F., Mehdipour, P., 2013. A comprehensive focus on global spectrum of BRCA1 and BRCA2 mutations in breast cancer. BioMed Res. Int. 21 2013.

Karran, P., 2000. DNA double strand break repair in mammalian cells. Curr. Opin. Genet. Dev. 10 (2), 144–150.

Khanna, K.K., Keating, KE, Kozlov, S, Scott, S, Gatei, M, Hobson, K, Taya, Y, Gabrielli, B, Chan, D, Lees-Miller, SP, Lavin, MF., 1998. ATM associates with and phosphorylates p53: mapping the region of interaction. Nat. Genet. 20 (4), 398–400.

Kuhne, M., Riballo, E, Rief, N, Rothkamm, K, Jeggo, PA, Löbrich, M., 2004. A double-strand break repair defect in ATM-deficient cells contributes to radiosensitivity. Cancer Res. 64 (2), 500–508.

LaBarge, M.A., Garbe, J.C., Stampfer, M.R., 2013. Processing of human reduction mammoplasty and mastectomy tissues for cell culture. J. Vis. Exp. 71.

Lacey, K.R., Jackson, P.K., Stearns, T., 1999. Cyclin-dependent kinase control of centrosome duplication. Proc. Natl. Acad. Sci. USA 96 (6), 2817–2822.

Lee, J.K., Garbe, J.C., Vrba, L, Miyano, M., Futscher, B.W., Stampfer, M.R., LaBarge, M.A., 2015. Age and the means of bypassing stasis influence the intrinsic subtype of immortalized human mammary epithelial cells. Front. Cell Dev. Biol. 3, 13.

Mann, G.J., Thorne, H, Balleine, RL, Butow, PN, Clarke, CL, Edkins, E, Chenevix-Trench, G., 2006. Analysis of cancer risk and BRCA1 and BRCA2 mutation prevalence in the kConFab familial breast cancer resource. Breast Cancer Res. 8 (1), R12.

Mantel, C., Braun, SE, Reid, S, Henegariu, O, Liu, L, Hangoc, G, Broxmeyer, HE., 1999. p21(cip-1/waf-1) deficiency causes deformed nuclear architecture, centriole overduplication, polyploidy, and relaxed microtubule damage checkpoints in human hematopoietic cells. Blood 93 (4), 1390–1398.

Matsumoto, Y., Hayashi, K., Nishida, E., 1999. Cyclin-dependent kinase 2 (Cdk2) is required for centrosome duplication in mammalian cells. Curr. Biol. 9 (8), 429–432.

Matsuoka, S., Rotman, G, Ogawa, A, Shiloh, Y, Tamai, K, Elledge, SJ., 2000. Ataxia telangiectasia-mutated phosphorylates Chk2 in vivo and in vitro. Proc. Natl. Acad. Sci. USA 97 (19), 10389–10394.

Maxwell, K.N., Domchek, SM, Nathanson, KL, Robson, ME., 2016. Population frequency of germline BRCA1/2 mutations. J. Clin. Oncol. 34 (34), 4183–4185.

McDermott, K.M., Zhang, J, Holst, CR, Kozakiewicz, BK, Singla, V, Tlsty, TD, 2006. p16INK4a prevents centrosome dysfunction and genomic instability in primary cells. PLoS Biol. 4 (3), E51.

Meraldi, P., et al., 1999. Centrosome duplication in mammalian somatic cells requires E2F and Cdk2-cyclin A. Nat. Cell Biol. 1 (2), 88–93.

Meraldi, P., Nigg, E.A., 2002. The centrosome cycle. FEBS Lett. 521 (1–3), 9–13.

Moynahan, M.E., Chiu, JW, Koller, BH, Jasin, M., 1999. Brca1 controls homology-directed DNA repair. Mol. Cell 4 (4), 511–518.

Nigg, E.A., 2006. Origins and consequences of centrosome aberrations in human cancers. Int. J. Cancer 119 (12), 2717–2723.

Patel, K.J., Yu, VP, Lee, H, Corcoran, A, Thistlethwaite, FC, Evans, MJ, Colledge, WH, Friedman, LS, Ponder, BA, Venkitaraman, AR., 1998. Involvement of Brca2 in DNA repair. Mol. Cell 1 (3), 347–357.

Paterson, M.C., Anderson, AK, Smith, BP, Smith, PJ., 1979. Enhanced radiosensitivity of cultured fibroblasts from ataxia telangiectasia heterozygotes manifested by defective colony-forming ability and reduced DNA repair replication after hypoxic gamma-irradiation. Cancer Res. 39 (9), 3725–3734.

Rivera-Rivera, Y., Saavedra, H.I., 2016. Centrosome - a promising anti-cancer target. Biologics 10, 167–176.

Sato, C., Kuriyama, R., Nishizawa, K., 1983. Microtubule-organizing centers abnormal in number, structure, and nucleating activity in x-irradiated mammalian cells. J. Cell Biol. 96 (3), 776–782.

Shafman, T., Khanna, KK, Kedar, P, Spring, K, Kozlov, S, Yen, T, Hobson, K, Gatei, M, Zhang, N, Watters, D, Egerton, M, Shiloh, Y, Kharbanda, S, Kufe, D, Lavin, MF., 1997. Interaction between ATM protein and c-Abl in response to DNA damage. Nature 387 (6632), 520–523.

Shen, K., Wang, Y, Brooks, SC, Raz, A, Wang, YA., 2006. ATM is activated by mitotic stress and suppresses centrosome amplification in primary but not in tumor cells. J. Cell. Biochem. 99 (5), 1267–1274.

Somasundaram, K., Zhang, H, Zeng, YX, Houvras, Y, Peng, Y, Zhang, H, Wu, GS, Licht, JD, Weber, BL, El-Deiry, WS., 1997. Arrest of the cell cycle by the tumour-suppressor BRCA1 requires the CDK-inhibitor p21WAF1/CiP1. Nature 389 (6647), 187–190.

Sridharan, D.M., Chappell, LJ, Whalen, MK, Cucinotta, FA, Pluth, JM., 2015. Defining the biological effectiveness of components of high-LET track structure. Radiat. Res. 184 (1), 105–119.

Sridharan, D.M., Enerio, S, LaBarge, MA, Stampfer, MM, Pluth, JM., 2017. Lesion complexity drives age related cancer susceptibility in human mammary epithelial cells. Aging 9 (3), 665–686.

Sudo, H., Garbe, J, Stampfer, MR, Barcellos-Hoff, MH, Kronenberg, A., 2008. Karyotypic instability and centrosome aberrations in the progeny of finite life-span human mammary epithelial cells exposed to sparsely or densely ionizing radiation. Radiat. Res. 170 (1), 23–32.

Swift, M., Morrell, D, Cromartie, E, Chamberlin, AR, Skolnick, MH, Bishop, DT., 1986. The incidence and gene frequency of ataxia-telangiectasia in the United States. Am. J. Hum. Genet. 39 (5), 573–583.

Tutt, A., Gabriel, A, Bertwistle, D, Connor, F, Paterson, H, Peacock, J, Ross, G, Ashworth, A., 1999. Absence of Brca2 causes genome instability by chromosome breakage and

loss associated with centrosome amplification. Curr. Biol. 9 (19), 1107–1110.
Walsh, M.F., Nathanson, KL, Couch, FJ, Offit, K., 2016. Genomic biomarkers for breast cancer risk. Adv. Exp. Med. Biol. 882, 1–32.
Wang, R.H., Yu, H., Deng, C.X., 2004. A requirement for breast-cancer-associated gene 1 (BRCA1) in the spindle checkpoint. Proc. Natl. Acad. Sci. USA 101 (49), 17108–17113.
Weeks, D.E., Paterson, MC, Lange, K, Andrais, B, Davis, RC, Yoder, F, Gatti, RA., 1991. Assessment of chronic gamma radiosensitivity as an in vitro assay for heterozygote identification of ataxia-telangiectasia. Radiat. Res. 128 (1), 90–99.
Weissberg, J.B., Huang, D.D., Swift, M., 1998. Radiosensitivity of normal tissues in ataxia-telangiectasia heterozygotes. Int. J. Radiat. Oncol. Biol. Phys. 42 (5), 1133–1136.
Xu, X., Weaver, Z, Linke, SP, Li, C, Gotay, J, Wang, XW, Harris, CC, Ried, T, Deng, CX., 1999. Centrosome amplification and a defective G2-M cell cycle checkpoint induce genetic instability in BRCA1 exon 11 isoform-deficient cells. Mol. Cell 3 (3), 389–395.
Zhou, B.B., Elledge, S.J., 2000. The DNA damage response: Putting checkpoints in perspective. Nature 408 (6811), 433–439.